Detection of Acute Respiratory Distress Syndrome using Sectoral Bioimpedance Spectroscopy – a Pilot Study

J. Orschulik[1], N. Hochhausen[2], S. Aguiar Santos[1], M. Czaplik[2], S. Leonhardt[1], M. Walter[1]

[1]Philips Chair for Medical Information Technology, Helmholtz Institute for Biomedical Engineering, RWTH Aachen University, Aachen, Germany

[2]Department of Anaesthesiology, University Hospital RWTH Aachen, Aachen, Germany

Contact: orschulik@hia.rwth-aachen.de

Introduction

Lung pathologies such as edema, atelectasis or pneumonea are life threatening conditions, especially in critically ill patients. When not diagnosed and treated in an early stage, these pathologies may even result in an Acute Respiratory Distress Syndrome (ARDS) [1]. Thus, a bedside available diagnostic tool would be highly recommended. Today, however, usually a combination of x-ray, blood gas analysis, computer tomography (CT) or sonography is used in order to detect such pathologies [2–4]. ARDS is classified using the Horowitz index, which measures the ratio of partial pressure of oxygen in blood and the fraction of oxygen in inhaled air (PaO_2 / FiO_2). A value between 200 mmHg and 300 mmHg describes a mild, a value between 100 mmHg and 200 mmHg a moderate and a value below 100 mmHg a severe ARDS [5]. The idea of this project is to use Bioimpedance Spectroscopy, a tool which is available at the bedside and showed promising results as a fluid management tool, to detect these pathologies [6]. In an earlier publication, we showed *ex-vivo* that it is possible to differentiate between blood and water content in the lung based on the impedance spectrum [7]. Furthermore, we developed measurement strategies utilizing both internal and external electrodes to focus bioimpedance measurements to specific regions of interest [8, 9]. In this paper, we present the first results of a pilot animal study investigating the possibility of bioimpedance spectroscopy for diagnosing ARDS.

Materials and Methods

Bioimpedance Spectroscopy

In general, the dielectric properties of body tissue are frequency dependent [10]. In bioimpedance applications, especially the so-called β-dispersion, which is caused by the cell membrane and typically occurs in the frequency range of a few kHz up to 1 MHz, is most prominent. Due to the polarization effect at the cell membrane, the current path through biological tissue depends on the current injection frequency. This is demonstrated in Fig. 1, left. At low frequencies, the main current flows around the cell membrane as it has a capacitive behavior. At higher frequencies, the current flows through both the extra- and the intracellular space. This behavior can be modeled and approximated using the equivalent circuit in Fig. 1, right. Bioimpedance Spectroscopy (BIS) exploits this by measuring the complex electrical impedance at different injection frequencies in the β-dispersion range. By analyzing the resulting frequency dependent, complex impedance, information about the body composition such as fat-free mass and total body water can be extracted [12].

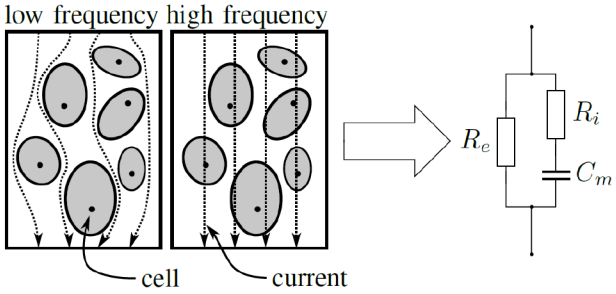

Figure 1: Current flow through biological tissue at low and high frequencies and electrical equivalent circuit (from [11]).

Animal Trial Setup

The experiment was performed in accordance with the German legislation governing animal studies following *The Principles of Laboratory Animal Care* and was approved by the North Rhine-Westphalia State Agency for Nature, Environment, and Consumer Protection (Germany; 84-02.04.2013.A200).

In this study, acute respiratory distress syndrome was induced in a female pig (German Landrace, *Sus scrofa*) weighing 36,6 kg. After induction of anesthesia, the animal was intubated and mechanically ventilated. General anesthesia was maintained during the entire trial. Subsequently, femoral arterial and central venous catheter as well as a pulmonary catheter were placed. Additionally, the impedance measurement devices were connected. After finishing the preparations, baseline impedance measurements were performed. Thereafter, ARDS was induced by an infusion of lipopolysaccharide (LPS) [13]. Three hours later, a mild ARDS (paO2/FiO2 201-300 mmHg) was observed. Henceforth, impedance measurements were collected hourly for 8 hours.

Measurement setup

In this study, bioimpedance spectroscopy measurements were performed using the BIS device *Sfb7* from Imped-

imed (Carlsbad, USA). Impedance was measured at 256 frequency points between 4 kHz and 1 MHz. The length of one spectroscopic impedance measurement took less than 1 second. A total of 18 electrodes (16 external and 2 internal) were used for bioimpedance measurements. Fig. 2 shows the positions of the electrodes. Electrodes 1–5 and

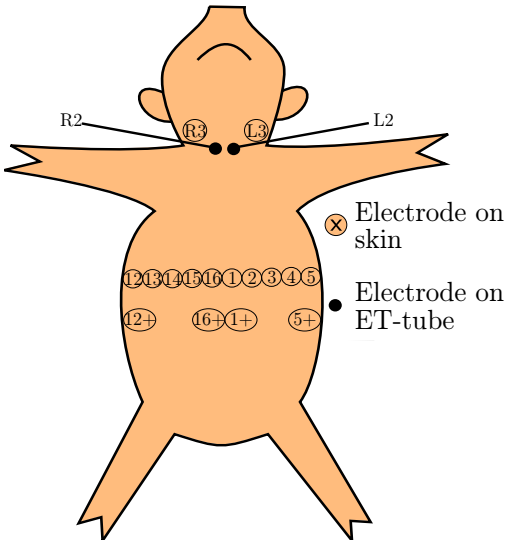

Figure 2: Electrode positions used in this study for different measurements setups. A total of eight different electrode configurations were used utilizing both internal and external electrodes.

12–16 were placed similar to the electrode positions used in Electrical Impedance Tomography at approx. the height of the 5th intercostal space. Electrodes 1+, 5+, 12+ and 16+ were placed approx. 10 cm below the corresponding electrodes 1, 5, 12 and 16. Electrodes L2 and R2 are internal electrodes inside the trachea. For those, a special endotracheal tube (provided by MicroPen Technologies, Honeoye Falls, NY, USA) with printed electrodes on the cuff was used. Fig. 3 shows a picture of this tube with

Figure 3: Endotracheal tube with integrated electrodes on the cuff used throughout this study.

internal electrodes. Finally, electrodes L3 and R3 were placed on the skin at the same height as the internal electrodes. Impedance measurements were performed hourly using eight different electrode configurations. Tab. 1 shows

Table 1: Electrode configurations used in this study. Measurements using eight different electrode configurations were performed. $i_{+/-}$ represents the electrode numbers of the current driving and $v_{+/-}$ the electrode numbers of the sensing electrode pairs, respectively.

Config #	i_+	i_-	v_+	v_-
1	4	13	5	12
2	L2	2	R2	15
3	L2	2	R3	3
4	R2	15	L3	14
5	L2	5	L3	4
6	R2	12	R3	13
7	16	12	16+	12+
8	1	5	1+	5+

the electrode numbers of the injecting and sensing electrode pairs, respectively. Location and selection of the electrodes were based on the results of a simulation study published in [8] and [9]. In the trial, both transthoracic configurations (config #1) and configurations focusing on different regions (config #2–8) were measured. However, the preliminary results presented in this paper will be based on the transthoracic configuration #1.

Results and Discussion

The results of the medical parameters are shown in Fig. 4. Both the progress of the lung compliance ($\Delta V/\Delta P$) and

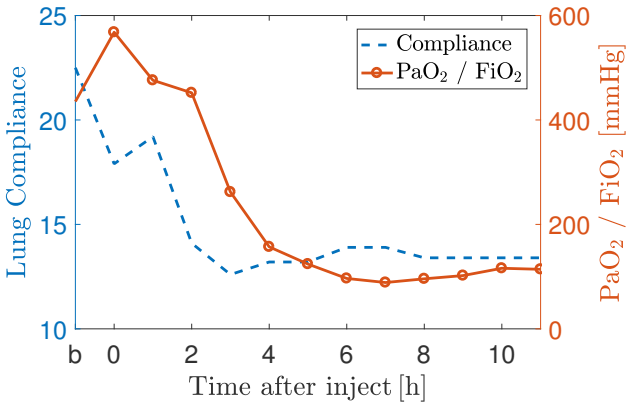

Figure 4: Medical data of the animal trial. The time after Lipopolysaccharid-injection is shown on the x-axis. "b" denotes the baseline measurement. The compliance is shown in blue and the Horowitz-index in red. 3 hours after injection, an ARDS was diagnosed (PaO_2 / FiO_2 < 300).

the Horowitz-index PaO_2 / FiO_2 are shown. First, it can be observed that animal model chosen in this study does indeed induce an Acute Respiratory Distress Syndrome. As mentioned earlier, ARDS is diagnosed if the Horowitz-index is below 300 mmHg. Three hours after LPS injection,

the Horovitz-index was 262 mmHg and the compliance decreased to 12.6 ml/mbar. In conclusion, the animal suffered from a mild ARDS. While the compliance is available at bedside, blood gas analysis has to be performed to calculate the Horowitz-index.
In Fig. 5, the Horowitz-index is compared to the absolute

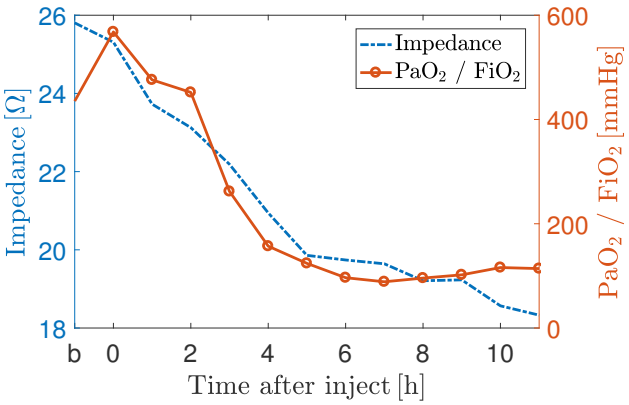

Figure 5: Absolute value of the measured impedance at configuration #1 at 70 kHz (blue) compared to the Horowitz-index (red). The time after Lipopolysaccharid-injection is shown on the x-axis. "b" denotes the baseline measurement. 3 hours after injection, an ARDS was diagnosed (PaO_2 / FiO_2 < 300).

value of the impedance at 70 kHz using electrode configuration #1. It is apparent that the absolute value decreases as the ARDS develops. Furthermore, the gradient of the absolute impedance decreases after t= 5 h which is consistent to the Howoritz-index. In both the Horowitz-index and the absolute impedance, the highest gradient occurs between t=2 h and t=5 h.
In Fig. 6, the absolute value of the impedance is shown from 10 kHz to 1 MHz. First, it can be seen that, in ac-

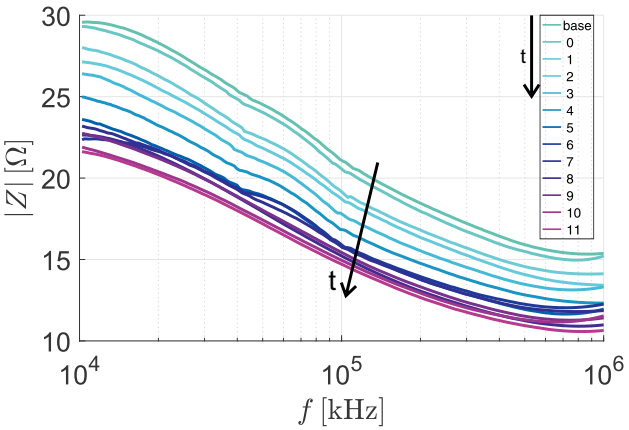

Figure 6: Absolute value of the impedance from 10 kHz to 1 MHz. It can be seen that the observed drop in impedance is present at all frequencies.

cordance to Fig. 1, the absolute value of the impedance is dependent on the frequency and is higher at low frequencies. Furthermore, it is also visible that the results from Fig. 5 are valid in the complete frequency range. The absolute value drops most in the first hours ($t < 5$ h) and stays in the same region once an ARDS has been established ($t \geq 5$ h). However, this impedance drop is not constant throughout the complete frequency range. While at 10 kHz, the absolute value of the impedance drops approx. 8 Ω, it only drops approx. 5 Ω at 1 MHz. To analyze this further, in Fig. 7 the real and imaginary part of the spectroscopic measurement result is shown in the complex plane for each measurement point. The typical semicircular shape of the impedance spectrum is visible throughout the trial. While the real part of the impedance drops constantly, the imaginary part decreases at low frequencies and rises for higher frequencies. The minimum value of the imaginary part is frequency dependent and is found at approx. 70 kHz. Most important, however, again a cluster of similar impedance spectrums is visible from approx. t=5 h to t=11 h. When comparing this to the medical results in Fig. 4, this is also the span in which the Horowitz-index stayed in the same region. Thus, both the absolute values and the shape of the spectrum does not significantly change once an ARDS has been established.

Conclusions

In this paper, we demonstrated in a pilot study that an Acute Respiratory Distress Syndrome (ARDS) has an impact on Bioimpedance Spectroscopy measurements performed in the thoracic area. Using absolute impedance values, a high correlation between the Horowitz-index and the impedance value was observed. Additionally, the shape and individual values of the spectroscopic measurements were also dependent on the lung status. No technical difficulties were observed throughout the complete trial. However, no final statement on the possibility of the detection of ARDS based on the impedance spectrum can be made. While an impact on the impedance is apparent, many other factors such as the fluid volume of the animal, the temperature or the ventilation settings also have an influence on the measured impedance. Furthermore, the absolute values obtained in this trial are only valid for this specific animal. While it would be easy to state in this data that an absolute value of the measured transthoracic impedance at 70 kHz below 21 Ω is related to an ARDS, this threshold might be shifted in other trials. Consequently, in future work we will perform additional animal trials including both different pathologies such as edema and a control group without intervention. Based on this data, further analysis of the correlation between the impedance spectroscopy measurements and the medical data. Additionally, relative indices based on datapoints from all eight electrode configurations at different frequency points could be developed. Nevertheless, impedance spectroscopy is a promising technology for the detection of ARDS as it is available at bedside, non-harming, real time capable and comparatively affordable.

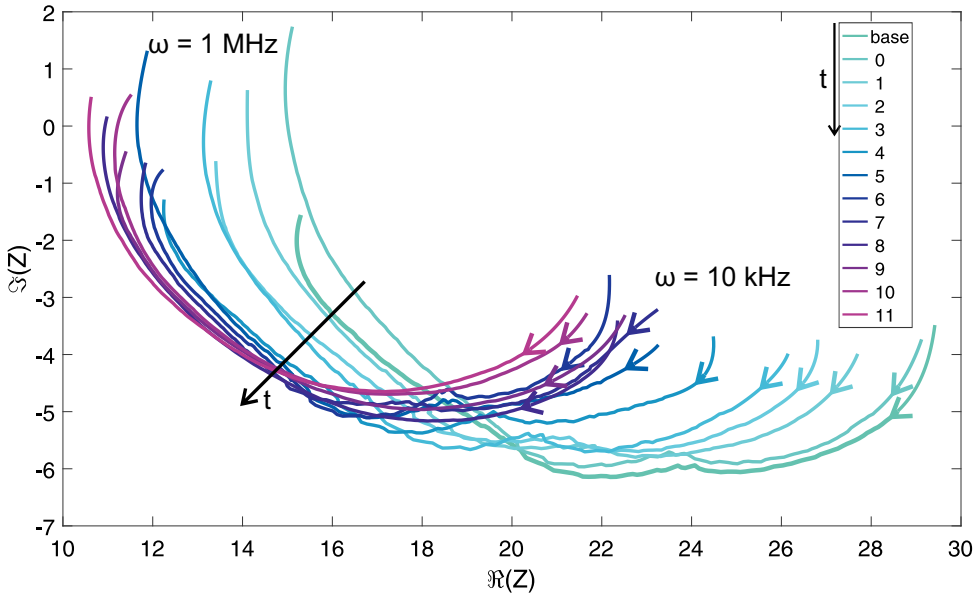

Figure 7: Results of the Bioimpedance Spectroscopy (BIS) measurements at configuration #1 (see Tab. 1). Both the real and imaginary part is shown as a function of the frequency. BIS was recorded at an hourly rate. A stable ARDS was diagnosed at t=3h (see Fig. 4.)

References

[1] B. Taylor Thompson, Rachel C. Chambers, and Kathleen D. Liu. Acute respiratory distress syndrome. *New England Journal of Medicine*, 377(6):562–572, aug 2017.

[2] C. H. Marquette, M. C. Copin, F. Wallet, R. Neviere, F. Saulnier, D. Mathieu, A. Durocher, P. Ramon, and A. B. Tonnel. Diagnostic tests for pneumonia in ventilated patients: prospective evaluation of diagnostic accuracy using histology as a diagnostic gold standard. *Am J Respir Crit Care Med*, 151(6):1878–1888, Jun 1995.

[3] American Thoracic Society and Infectious Diseases Society of America. Guidelines for the management of adults with hospital-acquired, ventilator-associated, and healthcare-associated pneumonia. *American Journal of Respiratory and Critical Care Medicine*, 171(4):388–416, feb 2005.

[4] Ali Nawaz Khan, Hamdan Al-Jahdali, Sarah Al-Ghanem, and Alaa Gouda. Reading chest radiographs in the critically ill (part ii): Radiography of lung pathologies common in the icu patient. *Ann Thorac Med*, 4(3):149–157, Jul 2009.

[5] The ARDS Definition Task Force. Acute respiratory distress syndrome. *JAMA*, 307(23), jun 2012.

[6] Sören Weyer, Matthias Daniel Zink, Tobias Wartzek, Lennart Leicht, Karl Mischke, Thomas Vollmer, and Steffen Leonhardt. Bioelectrical impedance spectroscopy as a fluid management system in heart failure. *Physiological Measurement*, 35(6):917–930, Jun 2014.

[7] Nadine Hochhausen, Jakob Orschulik, Susana Aguiar Santos, Steffen Leonhardt, and Michael Czaplik. Determination of lung pathology by multi-frequent analysis. *17th International Conference on Electrical Impedance Tomography. Stockholm, Sweden, June 19th – 23rd*, 2016.

[8] Jakob Orschulik, Rudolf Petkau, Tobias Wartzek, Nadine Hochhausen, Michael Czaplik, Steffen Leonhardt, and Daniel Teichmann. Improved electrode positions for local impedance measurements in the lung—a simulation study. *Physiological Measurement*, 37(12):2111–2129, nov 2016.

[9] Jakob Orschulik, Nadine Hochhausen, Michael Czaplik, Daniel Teichmann, Steffen Leonhardt, and Marian Walter. Addition of internal electrodes is beneficial for focused bioimpedance measurements in the lung. *Physiological Measurement*, feb 2018.

[10] S. Gabriel, R. W. Lau, and C. Gabriel. The dielectric properties of biological tissues: Ii. measurements in the frequency range 10 hz to 20 ghz. *Phys Med Biol*, 41(11):2251–2269, Nov 1996.

[11] Thomas Schlebusch, Lisa Röthlingshöfer, Saim Kim, Marcus Köny, and Steffen Leonhardt. On the road to a textile integrated bioimpedance early warning system for lung edema. In *2010 International Conference on Body Sensor Networks*. Institute of Electrical and Electronics Engineers (IEEE), jun 2010.

[12] UG. Kyle, I. Bosaeus, AD. De Lorenzo, P. Deurenberg, M. Elia, JM. Gómez, BL. Heitmann, L. Kent-Smith, JC. Melchior, M. Pirlich, H. Scharfetter, AM. Schols, C. Pichard, and Composition of the ESPEN Working Group. Bioelectrical impedance analysis - part i: review of principles and methods. *Clinical Nutrition*, 23(5):1226–1243, October 2004.

[13] H.M. Wang, M. Bodenstein, and K. Markstaller. Overview of the pathology of three widely used animal models of acute lung injury. *European Surgical Research*, 40(4):305–316, 2008.

Acknowledgments

The authors gratefully acknowledge financial support provided by the German Research Foundation [Deutsche Forschungsgemeinschaft (DFG), LE 817/20-1, CZ 215/2-1].